

An Exploration of the Effects of Periodic Top Predator Interference and Hunting on a Predator-Prey System

Original

An Exploration of the Effects of Periodic Top Predator Interference and Hunting on a Predator-Prey System / Acotto, F., Bardi, L., Manzini, A., Sarfatti, O., Viscardi, A., Venturino, E. - In: Trends in Biomathematics: Exploring Epidemics, Eco-Epidemiological Systems, and Optimal Control StrategiesELETTRONICO. - [s.l.] : Springer, 2024. - ISBN 9783031590719. - pp. 277-297 [10.1007/978-3-031-59072-6_14]

Availability:

This version is available at: 11583/2990533 since: 2024-07-11T19:46:28Z

Publisher:

Springer

Published

DOI:10.1007/978-3-031-59072-6_14

Terms of use:

This article is made available under terms and conditions as specified in the corresponding bibliographic description in the repository

Publisher copyright

(Article begins on next page)

**AN EXPLORATION OF THE EFFECTS OF PERIODIC TOP
PREDATOR INTERFERENCE AND HUNTING ON A
PREDATOR-PREY SYSTEM ***

FRANCESCA ACOTTO, LEONARDO BARDI, ALESSANDRO MANZINI,
OLIVIA SARFATTI, ALBERTO VISCARDI[†] AND EZIO VENTURINO[†]

*Dipartimento di Matematica “Giuseppe Peano”,
Università di Torino,*

via Carlo Alberto 10, 10123 Torino, ITALY

[†]Member of the INdAM research group GNCS

*E-mail: francesca.acotto@unito.it, leonardobardi33@gmail.com,
lmanzinialessandro@gmail.com, olli_oi@tiscali.it, alberto.viscardi@unito.it,
ezio.venturino@unito.it*

We introduce two models for the investigation of damages that periodic passages of migrating animals may have on established ecosystems of a smaller scale. In the first one, the damage is only of “physical” nature, in which the population at the highest trophic layer ravages the territory where the other interacting species live, thereby reducing their survival capabilities but not obtaining any benefit out of this. In the second one, it is assumed that the periodic damage comes from a moving top predator, periodically crossing the habitat of the lower trophic level populations, chasing both of them and therefore getting a reward from this hunt. The underlying model is assumed to be of minimalist predator-prey type, in order to better elucidate the effect of the action of the top predator. While the pure interference model does not seem to produce relevant effects other than the presence in a two-dimensional subspace of neutrally stable trajectories, a behavior that is forbidden in the underlying basic predator-prey model, the superpredation of a migrating population in suitable conditions induces a stable equilibrium, which may undergo a Hopf bifurcation with specific parameter choices. This elementary investigation elucidates therefore a possible invasion mechanism where the migrating population spots an attracting ecosystem in which thriving is possible and settles in it, substantially altering it and affecting the native populations.

*Work partially supported by the project “Metodi di approssimazione e modelli per le scienze della vita” of the Dipartimento di Matematica “Giuseppe Peano”.

1. Introduction

Animal migration can be driven by multiple factors, including movement to hospitable environments when local conditions become unfavorable [1–3]. Migrating animals often move together, sometimes in large numbers [4, 5]. The most famous and most studied migratory movements are certainly those of birds [6–8], especially hoopoes (*Upupa epops*), swallows (*Hirundo rustica*) and storks (*Ciconia ciconia*). However, the phenomenon of migration actually affects other classes of the animal kingdom as well, among them we have also mammals [9–11]. Migratory movements have been analyzed in the literature also in mathematical terms, in particular the dynamics of different migrant populations have been modeled [17–22].

In this paper, we intend to investigate the dynamics of a specific phenomenon that occurs frequently in wild areas. Large mammal populations, especially herbivores, move seeking new and better pastures, and are often followed by their predators [12, 13]. The game paths employed in this search may disrupt the living environment of other species, most likely of smaller size, thereby indirectly reducing their habitat size and consequently their thriving conditions [14, 15]. In addition, the migrating populations could be exploiters of the resources at the lower trophic levels, not just damaging their environment [16].

We address both situations in order to understand the differences of the damages due to the different migrators' behaviors. Namely, we introduce two models for the investigation of disturbances induced by the periodic passages of migrating populations. In the first one, the population at the highest trophic layer ravages the territory where the other interacting species live, but does not obtain any benefit out of this action. In the second one, it is assumed that the the moving population acts as a top predator, periodically crossing the habitat of the lower trophic level populations, chasing both of them and therefore getting a reward from this hunt [23, 24].

The underlying model is assumed to be of minimalist predator-prey type, in order to better elucidate the effect of the action of the top predator. The latter is modeled via a periodic function of the population itself, thus it is of endogenous type. This allows us to investigate still an autonomous system and not one in which an exogenous forcing function of time is present, that renders the differential system nonautonomous.

The paper is organized as follows. In Section 2 we summarize the basic properties of the classical predator-prey system at the lowest trophic level.

Section 3 contains the larger system with the migrating population inducing only damages for the lower level ecosystem. In Section 4 the attention is instead focused on the superpredation. This is followed by a section containing numerical simulations and a section of discussion. Finally, a conclusion section ends the paper.

2. The basic underlying model

To begin with, for later comparison purposes, we consider a classical basic predator-prey system of the form

$$\begin{aligned}\frac{dP}{dt} &= sP - aPH, \\ \frac{dH}{dt} &= rH \left(1 - \frac{H}{k}\right) + \alpha PH.\end{aligned}\tag{1}$$

Here P represent the prey reproducing with Malthus rate s , therefore assuming that an unlimited supply of food is available for this population. The facultative predators H have instead reproduction rate r and carrying capacity k , from other resources not explicitly modeled. Further, a denotes the hunting rate and α is the corresponding benefit for the predators.

Its Jacobian is

$$J = \begin{pmatrix} s - aH & -aP \\ \alpha H & r - 2\frac{r}{k}H + \alpha P \end{pmatrix}.$$

This classical system allows only three equilibria, the origin \tilde{E}_0 , which is unconditionally feasible but unstable, in view of the Jacobian's eigenvalues s and r , the prey-free equilibrium $\tilde{E}_1 = (0, \tilde{H}_1) = (0, k)$, and coexistence $\tilde{E}_* = (\tilde{P}_*, \tilde{H}_*)$, where

$$\tilde{H}_* = \frac{s}{a} \quad \text{and} \quad \tilde{P}_* = \frac{r}{\alpha} \left(\frac{s}{ak} - 1 \right).$$

\tilde{E}_1 is unconditionally feasible. The stability condition for \tilde{E}_1 , namely

$$\rho := \frac{s}{ak} < 1,\tag{2}$$

is the opposite one for the feasibility of \tilde{E}_* , i.e.

$$\rho \geq 1.\tag{3}$$

Furthermore, at \tilde{E}_* the trace of the Jacobian is negative and its determinant is positive,

$$\text{tr}(J(\tilde{E}_*)) = -\frac{r}{k}\tilde{H}_* < 0, \quad \det(J(\tilde{E}_*)) = \alpha a \tilde{P}_* \tilde{H}_* > 0.$$

The fact that the trace cannot vanish for suitable parameter combinations shows that Hopf bifurcations cannot occur. Further, the Routh-Hurwitz conditions being satisfied unconditionally implies that coexistence, when feasible, is locally asymptotically stable. Being the only viable equilibrium in such case, it is also globally asymptotically stable.

Furthermore, in view of (2) and (3), the two equilibria are related to each other via a transcritical bifurcation. Hence, the dynamics is completely regulated by the value of the prey invading parameter ρ , for which when the latter crosses from below the critical threshold 1, the prey establish themselves in the ecosystem, with \tilde{E}_* emerging from the equilibrium \tilde{E}_1 .

3. The model for landscape disruption

Here we introduce periodic migration of the superpredator population A into (1). The migrating population is thus modeled via

$$\frac{d^2 A}{dt^2} + \omega^2(A - A_0) = 0. \quad (4)$$

In this situation, we temporarily disregard any possible vital dynamics for the migrating population. Hence, it is of constant size. The fluctuation modeled by the above equation concerns only its larger or smaller presence in the environment where the predator-prey system at a lower trophic level thrives. This assumption will be removed later on in the second model where demographics will be considered also for the superpredator. This feature is studied because at the moment we would like to assess only the damages caused to the underlying predator-prey system, disregarding possible benefits for the migrating superpredator. Hence, the full system gets modified as follows

$$\begin{aligned} \frac{dP}{dt} &= sP - aPH - bPA, \\ \frac{dH}{dt} &= rH \left(1 - \frac{H}{k}\right) + \alpha PH - \beta HA, \\ \frac{dA}{dt} &= Y, \\ \frac{dY}{dt} &= -\omega^2(A - A_0). \end{aligned} \quad (5)$$

The first three possible equilibria are $E_0 = (0, 0, A_0, 0)$, which is unconditionally feasible,

$$E_1 = (0, H_1, A_0, 0) \quad \text{and} \quad E_2 = \left(P_2, 0, \frac{s}{b}, 0\right), \quad (6)$$

where

$$H_1 = \frac{k}{r} (r - \beta A_0).$$

For the equilibrium E_2 , P_2 is arbitrary, but we have a very strong feasibility condition, i.e., $A_0 = s/b$. Due to the restrictive nature of this condition, the existence of E_2 is extremely sensitive to parameter variations and thus it can be neglected in the analysis.

The coexistence of the four dependent variables is not possible. However, there exists an equilibrium containing the three real populations of interest, namely,

$$E_* = (P_*, H_*, A_0, 0),$$

where

$$H_* = \frac{s - bA_0}{a} \quad \text{and} \quad P_* = \frac{1}{\alpha} \left(\frac{rH_*}{k} + \beta A_0 - r \right).$$

Feasibility condition for E_1 is

$$r \geq \beta A_0, \quad (7)$$

while for E_* we have

$$s \geq bA_0 \quad \wedge \quad s \geq bA_0 + a \frac{k}{r} (r - \beta A_0), \quad (8)$$

that is

$$s \geq \max \left\{ bA_0, bA_0 + a \frac{k}{r} (r - \beta A_0) \right\}. \quad (9)$$

The Jacobian of (5) is

$$J = \begin{pmatrix} s - aH - bA & -aP & -bP & 0 \\ \alpha H & r - 2\frac{r}{k}H + \alpha P - \beta A & -\beta H & 0 \\ 0 & 0 & 0 & 1 \\ 0 & 0 & -\omega^2 & 0 \end{pmatrix}. \quad (10)$$

The block of zeros on the bottom left corner implies that the characteristic equation factorizes into the product of two quadratic equations, the second one giving conjugate pure imaginary eigenvalues, $\pm\omega i$, implying that in the $A - Y$ subspace the system behaves like a center, as expected. Consequently, we have neutral oscillations of the migrating population in the $A - Y$ subspace. These oscillations, in turn, also affect the populations of the original ecosystem, P and H , unless these ones vanish. Note that the

migrating population appears in the first two model equations in the two interference terms and therefore its fluctuations influence both P and H .

Now, for the remaining minor, at E_0 we find two explicit eigenvalues, $s - bA_0$ and $r - \beta A_0$ from which for these neutral oscillations the “stability” conditions follow, with respect to behavior in the $P - H$ subspace:

$$s < bA_0 \quad \text{and} \quad r < \beta A_0. \quad (11)$$

Hence, in the condition (11), trajectories in the four-dimensional phase space will approach the ones pertaining to the center found in the $A - Y$ subspace and the system will settle to these persistent oscillations.

At E_1 the upper left minor provides two explicit eigenvalues,

$$s - aH_1 - bA_0 \quad \text{and} \quad -\frac{r}{k}H_1 < 0. \quad (12)$$

Thus, we obtain the “stability” condition

$$s < bA_0 + aH_1,$$

which explicitly becomes

$$s + \frac{\beta}{r}akA_0 < ak + bA_0. \quad (13)$$

Again, the system settles to neutral oscillations in the $A - Y$ subspace when these conditions are satisfied.

At E_* , for the upper left 2×2 minor $J^\#$ of J , we have that the top right element vanishes and the other entries are

$$J_{12}^\#(E_*) = -aP_*, \quad J_{21}^\#(E_*) = \alpha H_*, \quad \text{and} \quad J_{22}^\#(E_*) = -\frac{r}{k}H_*.$$

Thus

$$\text{tr}(J^\#(E_*)) = -\frac{r}{k}H_* < 0 \quad \text{and} \quad \det(J^\#(E_*)) = a\alpha H_* P_* > 0. \quad (14)$$

This is enough to ensure that the Routh-Hurwitz conditions hold. We therefore conclude that the trajectories once again tend to neutral oscillations in the $A - Y$ subspace.

Now, we can observe that the second condition in (8) for the coexistence feasibility can be rewritten as

$$r(bA_0 + ak - s) \leq ak\beta A_0,$$

while the condition (13) for the “stability” of E_1 is equivalent to

$$r(bA_0 + ak - s) > ak\beta A_0.$$

These are two complementary conditions. The first one is always true when

$$s \geq bA_0 + ak, \quad (15)$$

whereas, alternatively, when

$$s < bA_0 + ak \quad (16)$$

is verified if and only if

$$r \leq r^\dagger := \beta A_0 \frac{ak}{bA_0 + ak - s}.$$

In contrast, the second one is never verified when (15) holds, whereas, alternatively, when (16) is satisfied, it is verified for $r > r^\dagger$.

Consequently, we can distinguish the following situations as the prey reproduction rate s varies.

- (1) If $s < bA_0$ the system goes toward oscillations around the non-zero components of E_0 , when $r < \beta A_0$, or E_1 , when $r \geq \beta A_0$.
- (2) Then, if $bA_0 \leq s < bA_0 + ak$ the populations move in the direction of E_1 , when $r > r^\dagger$, or E_* , when $r \leq r^\dagger$, settling toward persistent fluctuations around the non-zero equilibrium components.
- (3) Finally, if $s \geq bA_0 + ak$ the system exhibits periodic oscillations around the first three components of E_* .

Defining the additional parameters as follows:

$$\sigma := \frac{s}{bA_0}, \quad \sigma^\dagger := \frac{ak}{bA_0} \quad \text{and} \quad \rho := \frac{r}{\beta A_0}, \quad (17)$$

we can collect all possible behaviour of the system in Table 1.

	$\rho \in [0, 1)$	$\rho \in [1, \max\{1, \frac{\sigma^\dagger}{1+\sigma^\dagger-\sigma}\}]$	$\rho \in (\max\{1, \frac{\sigma^\dagger}{1+\sigma^\dagger-\sigma}\}, +\infty)$
$\sigma \in [0, 1)$	oscillations around E_0	oscillations around E_1	oscillations around E_1
$\sigma \in [1, 1 + \sigma^\dagger)$	oscillations around E_*	oscillations around E_*	oscillations around E_1
$\sigma \in [1 + \sigma^\dagger, +\infty)$	oscillations around E_*	oscillations around E_*	oscillations around E_*

Hence, in the first two cases, the dynamics is completely regulated by the predator reproduction rate r . When its value crosses the critical threshold,

which is βA_0 in the first case and r^\dagger in the second one, the predators H or the prey P establish themselves in the ecosystem, respectively. In the first case, the oscillations around the non-zero components of E_1 emerge from those around the third component of E_0 . The situation is similar in the second case for the equilibria E_* and E_1 . In the third one, instead, the system dynamics is independent of the value of r because we always have periodic attractive coexistence oscillations.

4. The model for periodic superpredation

Here we account for periodic migrations, in which both populations at the lower trophic level become food for the superpredator, for which we further assume vital dynamics. The migrating population is therefore assumed to be gaining a benefit at rate γ for feeding on these two populations, with no other external resources, and experiencing a natural mortality rate m . This fact is expressed by

$$\frac{dA}{dt} = \gamma A(P + H) - mA.$$

On the other hand, we should also consider that the presence of this predator in the ecosystem is periodic. To take it into account, we differentiate the above equation and add the contribution of the periodic migration, obtaining

$$\frac{d^2A}{dt^2} = \gamma \left[\frac{dA}{dt}(P + H) + A \left(\frac{dP}{dt} + \frac{dH}{dt} \right) \right] - m \frac{dA}{dt} - \omega^2(A - A_0).$$

Using this expression in the last equation of (5) we obtain its following variant

$$\begin{aligned} \frac{dP}{dt} &= sP - aPH - bPA, \\ \frac{dH}{dt} &= rH \left(1 - \frac{H}{k} \right) + \alpha PH - \beta HA, \\ \frac{dA}{dt} &= Y, \\ \frac{dY}{dt} &= \gamma Y(P + H) - mY - \omega^2(A - A_0) \\ &\quad + \gamma A \left[sP - aPH - bPA + rH \left(1 - \frac{H}{k} \right) + \alpha PH - \beta HA \right]. \end{aligned} \tag{18}$$

The possible equilibria must have $Y = 0$ to satisfy the third equilibrium equation. We find again some points already discovered in the first model

(5), namely $E_0 = (0, 0, A_0, 0)$, unconditionally feasible, and (6) with the same feasibility condition (7) for E_1 and the fact that we can disregard E_2 in the equilibria analysis since it disappears under slight parameter changes.

For the three-population equilibrium \widehat{E}_* in which Y vanishes, we find

$$\widehat{H}_* = \frac{s - b\widehat{A}_*}{a} \quad \text{and} \quad \widehat{P}_* = \frac{1}{\alpha} \left(\frac{r\widehat{H}_*}{k} + \beta\widehat{A}_* - r \right),$$

from the first and second equilibrium equations, respectively. Substituting of the values of \widehat{H}_* and \widehat{P}_* into the last equilibrium equation yields again $\widehat{A}_* = A_0$. Hence, this equilibrium coincides with E_* of the previous model (5) and therefore has the same feasibility condition (9).

For the stability, note that the Jacobian (10) of (5) is partially modified. Its last row now becomes

$$\begin{aligned} J_{41} &= \gamma Y + \gamma A[s - bA + (\alpha - a)H], \\ J_{42} &= \gamma Y + \gamma A \left[(\alpha - a)P + r \left(1 - \frac{2H}{k} \right) - \beta A \right], \\ J_{43} &= -\omega^2 - \gamma A(bP + \beta H) \\ &\quad + \gamma \left[sP - aPH - bPA + rH \left(1 - \frac{H}{k} \right) + \alpha PH - \beta HA \right], \\ J_{44} &= \gamma(P + H) - m. \end{aligned}$$

At the equilibrium E_0 for the bottom right 2 by 2 subblock \widehat{J} , observe the simplifications

$$\widehat{J}_{43}(E_0) = -\omega^2 \quad \text{and} \quad \widehat{J}_{44}(E_0) = -m.$$

The 2 by 2 block on the left upper corner becomes a diagonal matrix, providing two explicit eigenvalues, $s - bA_0$ and $r - \beta A_0$, since the corresponding block in the right upper corner of J vanishes, so that the characteristic equation factorizes again. To investigate the behavior in the $A - Y$ subspace, we find

$$\text{tr}(\widehat{J}(E_0)) = -m < 0 \quad \text{and} \quad \det(\widehat{J}(E_0)) = \omega^2 > 0.$$

Hence, in this case, we do not have a center in the $A - Y$ subspace, but again the equilibrium is stable if (11) holds. Further, it is a stable node in the $A - Y$ subspace if

$$2\omega < m \tag{19}$$

10

and a stable focus conversely, given that the remaining eigenvalues are

$$\lambda_{\pm} = \frac{1}{2} \left[-m \pm \sqrt{m^2 - 4\omega^2} \right].$$

At E_1 one eigenvalue is immediately known, $s - aH_1 - bA_0$, giving rise to the same stability condition (13) of the corresponding equilibrium in the model (5). In the remaining minor, using the equilibrium equations, some simplifications occur:

$$\begin{aligned} J_{22}(E_1) &= -\frac{r}{k}H_1, & J_{23}(E_1) &= -\beta H_1, & J_{42}(E_1) &= -\gamma \frac{r}{k}A_0H_1, \\ J_{43}(E_1) &= -[\omega^2 + \beta\gamma H_1 A_0], & J_{44}(E_1) &= \gamma H_1 - m. \end{aligned}$$

The Routh-Hurwitz conditions for the remaining three-order minor \tilde{J} become

$$\text{tr}(\tilde{J}(E_1)) = -\frac{r}{k}H_1 - m + \gamma H_1 < 0,$$

which is

$$A_0 \beta r + \gamma k r < A_0 \beta \gamma k + r^2 + m r. \quad (20)$$

Then

$$\text{tr}(\tilde{J}(E_1))\tilde{M}_2 < \det(\tilde{J}(E_1))$$

must be satisfied, where the sum of the principal minors of order two is

$$\tilde{M}_2 = \omega^2 + \beta\gamma A_0 H_1 - \frac{r}{k}H_1(\gamma H_1 - m)$$

and the determinant is

$$\det(\tilde{J}(E_1)) = -\omega^2 \frac{r}{k}H_1 < 0.$$

Explicitly, in addition to (13), the stability conditions for E_1 in this model are (20) and

$$(m - \gamma H_1) \left(\omega^2 + \beta\gamma A_0 H_1 - \frac{r}{k}H_1 \left(\gamma H_1 - m - \frac{r}{k}H_1 \right) \right) + \frac{r}{k}\beta\gamma A_0 H_1^2 > 0. \quad (21)$$

Further, substitution of the values of H_1 into (21) and simplifications give

$$\begin{aligned} &(m - k\gamma) r^4 + ((k\gamma - m)^2 + 2(2k\gamma - m)\beta A_0) r^3 \\ &+ (((\beta A_0 - m)m + (5m - 5\beta A_0 - 4k\gamma)k\gamma)\beta A_0 - (k\gamma - m)\omega^2) r^2 \\ &+ ((2\beta A_0 + 5k\gamma - 3m)\beta A_0 + \omega^2) k\beta\gamma A_0 r \\ &- 2k^2\beta^3\gamma^2 A_0^3 > 0. \end{aligned} \quad (22)$$

At $\widehat{E}_* = E_*$ some of the entries of the Jacobian simplify:

$$\begin{aligned} J_{11}(\widehat{E}_*) &= 0, & J_{22}(\widehat{E}_*) &= -\frac{r}{k}H_*, \\ J_{41}(\widehat{E}_*) &= \alpha\gamma A_0 H_*, & J_{42}(\widehat{E}_*) &= -\gamma A_0 \left(\frac{r}{k}H_* + aP_* \right), \\ J_{43}(\widehat{E}_*) &= -\omega^2 - \gamma A_0 (bP_* + \beta H_*), & J_{44}(\widehat{E}_*) &= \gamma(P_* + H_*) - m. \end{aligned}$$

Considering the Routh-Hurwitz conditions for such a fourth-order Jacobian, the first one is

$$\text{tr}(J(\widehat{E}_*)) = -m + \gamma(P_* + H_*) - \frac{r}{k}H_* < 0,$$

giving the condition

$$m + \frac{r}{k}H_* > \gamma(P_* + H_*),$$

that is

$$((\gamma - \alpha)s + (\alpha - \gamma)bA_0 - ak\gamma) r + ((s\alpha + (a\beta - b\alpha)A_0)\gamma - am\alpha) k < 0. \quad (23)$$

Then, for the sum of the principal minors of order two, we get

$$\widehat{M}_2 = a\alpha H_* P_* - \frac{r}{k}H_* [\gamma(P_* + H_*) - m] + \omega^2 + \gamma A_0 (bP_* + \beta H_*).$$

For those of order three, we have

$$\begin{aligned} \widehat{M}_3 &= a\alpha P_* H_* (\gamma(P_* + H_*) - m) - b\alpha\gamma A_0 P_* H_* \\ &\quad - H_* \left(\frac{r}{k}(\omega^2 + \gamma A_0 (bP_* + \beta H_*)) - \beta\gamma A_0 \left(aP_* + \frac{r}{k}H_* \right) \right). \end{aligned}$$

Finally, the determinant is

$$\det(J(\widehat{E}_*)) = a\alpha\omega^2 P_* H_* > 0.$$

Since the determinant of $J(\widehat{E}_*)$ is positive, the stability is ensured by (23) and the further conditions

$$\widehat{M}_2 > 0, \quad \widehat{M}_3 > 0, \quad -\text{tr}(J(\widehat{E}_*))\widehat{M}_2 > \widehat{M}_3, \quad (24)$$

$$-\text{tr}(J(\widehat{E}_*))\widehat{M}_2\widehat{M}_3 > [\text{tr}(J(\widehat{E}_*))]^2 \det(J(\widehat{E}_*)) + (\widehat{M}_3)^2. \quad (25)$$

In conditions (24) and (25), we can substitute the first two coexistence equilibrium components. The expressions of the determinant, trace, and sum of principal minors of order two and order three become, respectively,

$$\det(J(\widehat{E}_*)) = \frac{\omega^2}{ak} (((bA_0 - 2s + ak) bA_0 + (s - ak) s) r - (bA_0 + s) ak\beta A_0),$$

12

$$\text{tr}(J(\widehat{E}_*)) = \frac{1}{ak\alpha} (((\gamma - \alpha)(s - bA_0) - ak\gamma)r + (s\alpha + (a\beta - b\alpha)A_0)k\gamma - a\alpha),$$

$$\widehat{M}_2 = \frac{\widehat{D}_2}{a^2k^2\alpha} \quad \text{and} \quad \widehat{M}_3 = \frac{\widehat{D}_3}{a^2k^2\alpha},$$

with

$$\begin{aligned} \widehat{D}_2 = & ((2s - ak - bA_0)bA_0 + (ak - s)s)\gamma r^2 \\ & + (((s + m - ak)a - \gamma s)s\alpha + (((\alpha - \gamma)a - \alpha\gamma)b + a\beta\gamma)bA_0^2)kr \\ & + (((ak - m - 2s)\alpha + (s - ak)\gamma)b - s\beta\gamma)a + 2bs\alpha\gamma)kA_0r \\ & + (((\gamma - \alpha)a - \alpha\gamma)bA_0 + (a + \gamma)s\alpha)\beta A_0 + a\alpha\omega^2)ak^2 \end{aligned}$$

and

$$\begin{aligned} \widehat{D}_3 = & ((5s - 3ak)bA_0 - 2b^2A_0^2 + (4s - ak)(ak - s))b\gamma A_0r^2 \\ & + ((ak - 2s)ak + s^2)s\gamma r^2 - (5\alpha b - 4a\beta)bk s\gamma A_0^2r \\ & - ((2b\alpha - 4a\beta)bA_0\gamma + (bm\alpha - (3(ak - s)\beta - 2\alpha bk)\gamma)ak)bA_0^2r \\ & - ((ks\gamma + \omega^2 + (s - ak)m)a - s^2\gamma)s\alpha r - 3bk s\alpha\gamma A_0r \\ & + (bm\alpha - (3(ak - s)\beta - 2bk\alpha)\gamma)akA_0r - bks^2\gamma\alpha A_0r \\ & + (ks\gamma + \omega^2 + (s - ak)m)abk\alpha A_0r - 2(a\beta - b\alpha)abk^2\beta\gamma A_0^3 \\ & + ((2(a\beta - b\alpha)s\gamma + (am - s\gamma)b\alpha)A_0 - (am - s\gamma)s\alpha)ak^2\beta A_0. \end{aligned}$$

5. Numerical simulations

On the basis of the results identified in the section 3, we can distinguish three cases for the model (5) as the prey reproduction rate s varies:

$$s < bA_0, \quad bA_0 \leq s < bA_0 + ak, \quad s \geq bA_0 + ak.$$

In the first two, the dynamics is completely regulated by the predator reproduction rate, while in the third one is univocally determined independently of r . Simulating the behavior of the system in each of these three cases, we have obtained the time series in Figures 1, 2 and in the left panel of Figure 3, respectively. The initial conditions are fixed at the values

$$P(0) = 0.8, \quad H(0) = 0.9, \quad A(0) = 0.6, \quad Y(0) = 0.2, \quad (26)$$

while the following reference parameter values are used:

$$a = 0.6, \quad b = 0.7, \quad k = 0.8, \quad \alpha = 0.2, \quad \beta = 0.4, \quad \omega = 1, \quad A_0 = 0.6. \quad (27)$$

The reproduction rates of prey and predators of the original ecosystem, instead, vary. In Figure 1, taking $s = 0.4$, we have considered $r = 0.2$ and $r = 0.4$. In Figure 2, fixing $s = 0.7$, we have used $r = 0.5$ and $r = 0.8$. Finally, in Figure 3, we have set $s = 1$ and $r = 0.6$. In all cases, we can observe that the system stabilizes at persistent oscillations around the non-zero components of the expected equilibrium points.

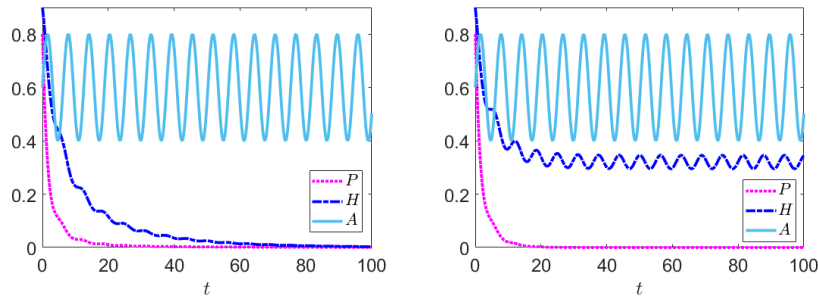


Figure 1. Oscillations of the system (5) around the non-zero components of the superpredator-only point E_0 and the prey-free equilibrium E_1 from the initial conditions (26), using the parameter values (27) and $s = 0.4$, with $r = 0.2$ (on the left) and $r = 0.4$ (on the right).

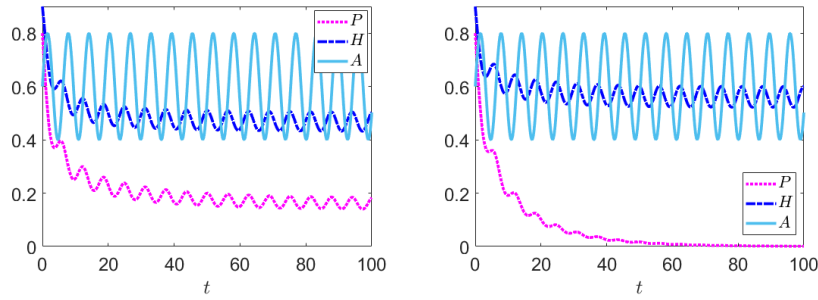


Figure 2. Oscillations of the system (5) around the non-zero components of coexistence E_* and the prey-free E_1 equilibria from the initial conditions (26), using the parameter values (27) and $s = 0.7$, with $r = 0.5$ (on the left) and $r = 0.8$ (on the right).

Specifically, in the first two cases, in which the behavior of the system (5) depends on the value of the parameter r , we have oscillations around the non-zero populations of one equilibrium emerging from those of another

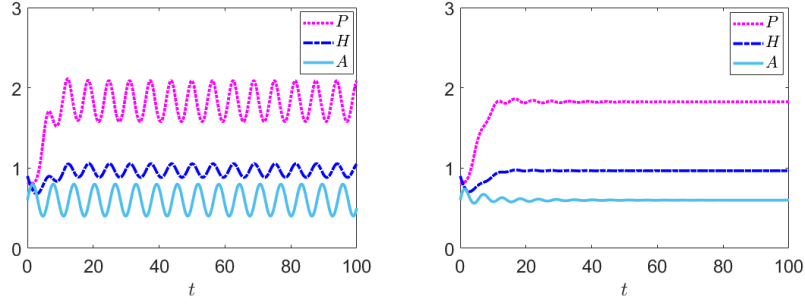


Figure 3. Oscillations of the system (5) around the non-zero components of the coexistence E_* (on the left) and achievement of this point by the system (18) (on the right) from the initial conditions (26), using the parameter values (27), (29), $s = 1$ and $r = 0.6$.

one. In the left panel of Figure 4 we can observe how predators H establish themselves in the ecosystem, when r crosses βA_0 , and similarly for prey P in the right one, when r goes below the threshold r^\dagger . In particular, as r varies from 0 to 1, the two diagrams in Figure 4 show the central values around which the populations fluctuate, if they do not vanish. These values are calculated as the arithmetic mean between the maximum value and the minimum value in a certain interval of integration times, when the situation has stabilized, namely between $t = 950$ and $t = 1000$. The initial conditions and parameter values, except r , are those of Figures 1 and 2.

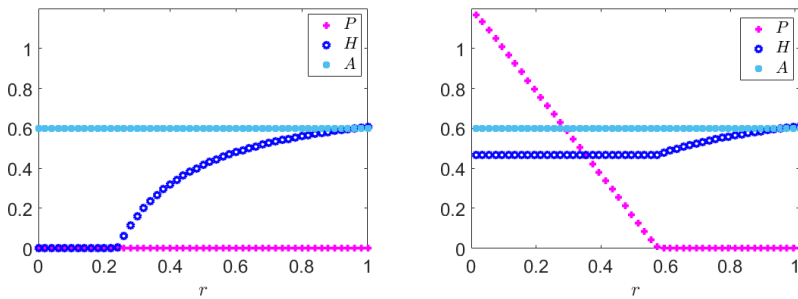


Figure 4. Transition of the system (5) from oscillations around the non-zero components of E_0 to those of E_1 , at $r = \beta A_0 = 0.240$, and from oscillations around the non-zero components of E_* to those of E_1 , at $r = r^\dagger = 0.576$. The initial conditions are (26). We fix $s = 0.4$ (on the left) and $s = 0.7$ (on the right) and we vary $r = 0 : 0.02 : 1$. The other parameter values are (27). In the case of non-zero equilibrium components, the heights of the plotted points are the central values around which the system fluctuates.

The oscillations of the model (5) around non-vanishing populations P and H of the original ecosystem are a consequence of the oscillations of the migrating population A . The equilibria are centers with closed orbits around them. The latter are uniquely determined by the parameters ω and A_0 for frequency and amplitude, but above all by the initial conditions $A(0)$ and $Y(0)$ that distinguish one trajectory from another one. The explicit solution of (4) is

$$A(t) = c_1 \cos(\omega t) + c_2 \sin(\omega t) + A_0, \quad c_1 = A(0) - A_0, \quad c_2 = \frac{Y(0)}{\omega}. \quad (28)$$

In Figure 5, starting from the initial conditions and parameter values of Figure 3, we have modified c_1 and c_2 , without altering A_0 , to observe how the migrating population oscillations of the coexistence equilibrium change, and consequently also oscillations of the populations P and H . Recalling (28), in particular we have considered $A(0) = 0.2$ to vary c_1 , in the left panel, $\omega = 2$ and $Y(0) = 0.1$ to vary c_2 , in the right one. In the former case, an increase in the oscillation amplitude is evident; in the latter, there is a significant contraction in amplitude and an increase in frequency. Clearly, keeping A_0 fixed, which is the third component of the equilibrium, the center of the migrating population oscillations remains the same in both cases.

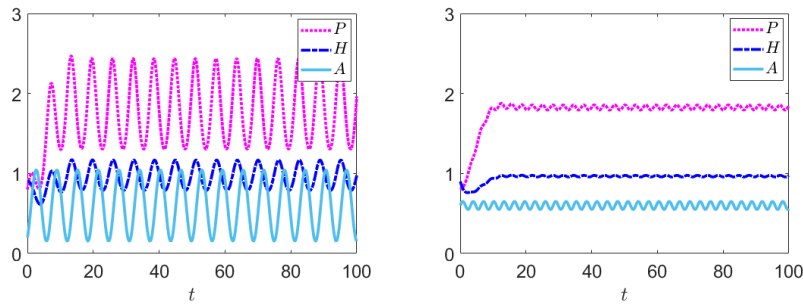


Figure 5. Oscillations of the system (5) around the non-zero components of the coexistence obtained by partially modifying the initial conditions and parameter values of Figure 3 as follows. Left panel: $A(0) = 0.2$. Right panel: $\omega = 2$ and $Y(0) = 0.1$.

Simulating the behavior of the system (18), using the initial conditions and parameter values of Figures 1, 2 and of the left panel of Figure 3, we have obtained that the populations stabilize at the same equilibria. Here,

unlike the case of the model (5), there are no neutrally persistent oscillations around the non-zero equilibrium components. For some populations, however, we can observe fluctuations just in the initial transient phase that damp out and fade away in time settling to the equilibrium point. The graphical results are reported in Figures 6, 7 and in the right panel of Figure 3, respectively. The additional parameter values are

$$\gamma = 0.3 \quad \text{and} \quad m = 0.9. \quad (29)$$

Thus, we have explicitly identified some examples in which the feasibility and stability conditions of the equilibrium points of the model (18) are simultaneously satisfied, thereby showing that these conditions are nonempty. These conditions are (7), (20), (22) for the prey-free equilibrium and (9), (23), (24), (25) for the coexistence one.

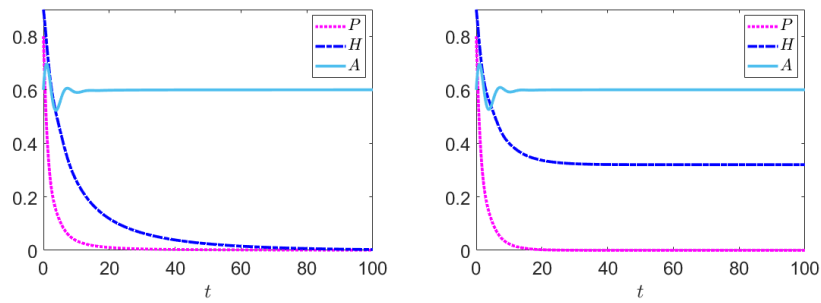


Figure 6. Superpredator-only and prey-free equilibria attained by the system (18) using the initial conditions and the parameter values of Figure (1), with in addition (29).

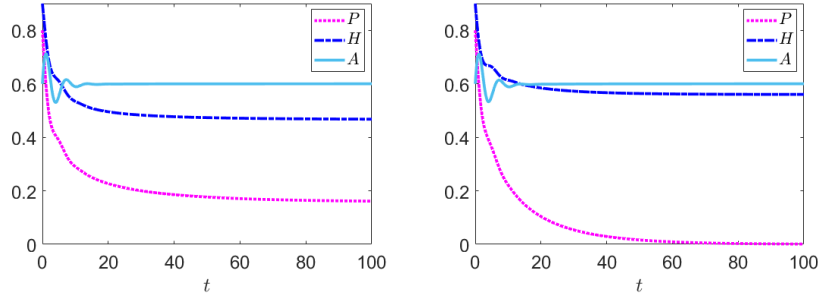


Figure 7. Coexistence and the prey-free equilibria reached by the system (18) using the initial conditions and the parameter values of Figure (2), with in addition (29).

The superpredator-only equilibrium around which we have the neutral oscillations in the left panel of Figure 1 is a center for the model (5) in the A - Y subspace, in agreement with the theoretical results of section 3. This is evident in Figure 8, where we can see the trajectories of the system (5) in the A - Y - $(P+H)$ space, on the left, from different initial conditions, and their projections in the A - Y subspace, on the right. The initial conditions that we have considered are (26),

$$P(0) = 0.4, \quad H(0) = 0.7, \quad A(0) = 0.4, \quad Y(0) = 0.5 \quad (30)$$

and

$$P(0) = 0.5, \quad H(0) = 0.2, \quad A(0) = 0.7, \quad Y(0) = 0.6. \quad (31)$$

For the model (18) with (29), as in the left panel of Figure 6, this equilibrium is instead a stable focus in the A - Y subspace, see Figure 9. In fact, the condition (19) is not verified. Changing the parameter values so that (19) is satisfied results in a stable node in the A - Y subspace, see Figure 10 with $\omega = 0.2$.

6. Discussion

6.1. The basic model

In the stated assumptions with unlimited prey food supply, the basic predator-prey model (1) can settle only to the prey-free environment or to coexistence, moving from one to the other one via a transcritical bifurcation governed by the parameter ρ , expressing prey invasion (2). This system also cannot persistently oscillate.

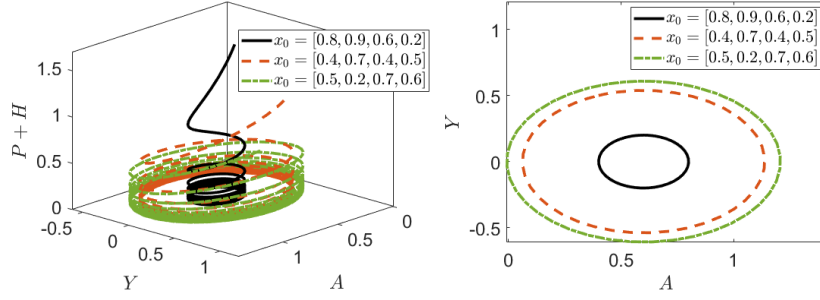


Figure 8. Trajectories of the system (5) in the A - Y - $(P + H)$ space (on the left), from the initial conditions (26), (30), (31), and their projections in the A - Y subspace (on the right). The parameter values are (27). The superpredator-only equilibrium is a center in the A - Y subspace.

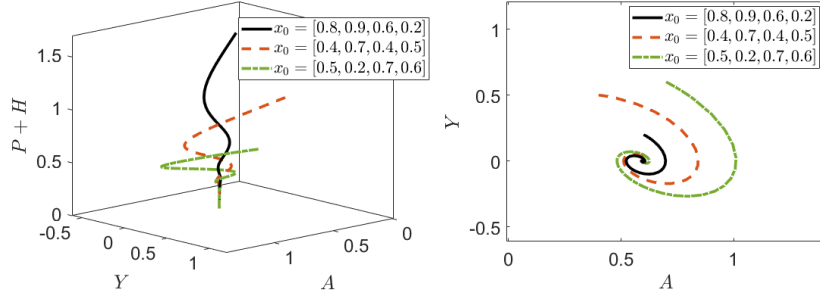


Figure 9. Trajectories of the system (18) in the A - Y - $(P + H)$ space (on the left), from the initial conditions (26), (30), (31), and their projections in the A - Y subspace (on the right). The parameter values are (27) and (29). The superpredator-only equilibrium is a stable focus in the A - Y subspace.

6.2. The interference model

The damages produced by the migrating population are accounted for in the model (5). Here the viable significant equilibria are three.

The first one E_0 is given by the migrating population at a constant level A_0 in the pristine environment, where both the underlying prey and predators are wiped out. This point corresponds to the origin, the equilibrium \tilde{E}_0 of (1), which however is unconditionally unstable. In order to attain E_0 , the reproduction rates of both prey and predators must be bounded above by the migrating population damaging rate, (11). This means that the underlying ecosystem is preserved, in the worst case at least in one of

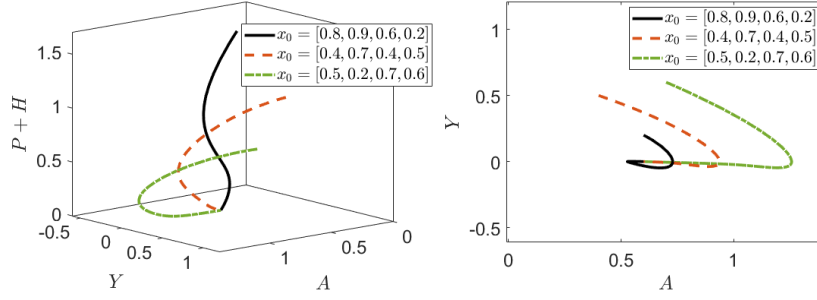


Figure 10. Trajectories of the system (18) in the A - Y - $(P+H)$ space (on the left), from the initial conditions (26), (30), (31), and their projections in the A - Y subspace (on the right). The parameter values are (27) and (29), but $\omega = 0.2$. The superpredator-only equilibrium is a stable node in the A - Y subspace.

its components, the predators, when no interference exists, but the damages of the migrating populations may drive it to extinction, in suitable conditions. Thus the unstable point \tilde{E}_0 of (1) remains the same, E_0 , but changes its stability nature when it is considered in the damaging model (5), through the action of the migrators. Around this point in the wider system (5), oscillations of neutral type exist, which have no counterpart in (1), as they are induced by the migrations. The migrating species thus wipes out the ecosystem and either continues to migrate over this territory (neutral orbits), or, most unlikely, settles in its place (at the level M_0) if the initial condition of its trajectory is exactly this value.

The point E_1 of (5) represents the corresponding prey-free equilibrium \tilde{E}_1 of (1). To attain it, we need to satisfy the condition (13) which is somewhat more involved than (2). And as for all the equilibria of (5), the point is a center in the $A - Y$ subspace. Further, by comparing the values of \tilde{H}_1 and H_1 , the latter is always below the former, so that the action of the migrators has a damaging effect on the predators of the underlying basic model. When (13) holds, orbits from the $P - H$ subspace are attracted toward the $A - Y$ one, in view of the fact that the two eigenvalues related to this subspace are real (12) and negative. This also prevents the occurrence of a Hopf bifurcation in the $P - H$ subspace.

The environment with the three populations always present can be attained, because the Routh-Hurwitz conditions hold unconditionally. In the $P - H$ subspace, note also that no persistent oscillations can arise, because the trace for no parameter values combinations vanishes, (14) forbidding the onset of a Hopf bifurcation there. The system trajectories tend then to

the neutrally stable cycles in the $A - Y$ subspace.

Note finally that both equilibria E_1 and E^* cannot sussist at the same time, as comparing the second condition in (8) and (13) we see that they are mutually exclusive and cannot hold simultaneously. Hence the system cannot have two different behaviors in two nonempty mutually exclusive subsets of the phase space.

In general, the action of the migrating population always reduces the equilibrium level of the prey of the underlying basic model, this is easily seen by comparing their values. For the predators instead, the reduction depends on the quantity

$$br - \beta ka \quad (32)$$

possibly being positive, as we can rewrite the equilibrium value of the predators as

$$P^* = \tilde{P}_* - \frac{A_0}{akr}(br - \beta ka).$$

We can interpret (32) being positive by rewriting it in the form

$$\frac{b}{a} > \frac{\beta}{r}.$$

The left-hand side represents the relative damage for the prey of the migrating species to the damage of their natural predators in the environment, while the right-hand side is the similar relative damage induced over these predators, over their interspecific competition rate. Hence in a relative sense, in this balance if the migrants affect more the prey P , their natural predators H gain, otherwise their population drops in view of the super-predator A hunting.

6.3. The superpredation model

The very same equilibria of model (5) are found here as well, with the same feasibility conditions, so that the considerations of the former subsection carry over here. Stability however needs more attention. Te major difference is found in the $A - Y$ subspace, where the equilibrium point E_0 becomes a node or a focus, depending on the condition (19). The stability conditions for both these points are more involved and difficult to interpret, but the bottom line is that a superpredation of a periodically migrating population induces the trajectories to settle toward a point in the three-dimensional subspace $P - H - A$ under suitable conditions, and not to neutrally stable cycles.

The most important consequence ensuing from the comparison of this superpredation model with the one of periodic damages is that in this case the coexistence equilibrium can be attained, in principle, if the suitable stability conditions are satisfied, while in the former one only periodic migrations are observed due to the neutrally periodic orbits of the system. This phenomenon corresponds to turning off the swinging migrant's presence, replacing it by a continuous presence in the environment. Hence a migrating population repeatedly crossing a habitat where it finds food and acceptable living conditions may settle permanently, invading and altering the underlying ecosystem.

7. Conclusion

We have presented two models describing the periodic passage of a population in an environment where a predator-prey system thrives. The models differ in their assumptions, because in the first one we account only for a disturbance of the underlying ecosystem, causing damages to both its populations without any gain for the migrating one; in the second one, the superpredator feeds on both populations at the lower trophic level during its presence in their environment.

The main changes induced by the migrating species are the oscillations that are found in both variants and are intrinsic in this assumption. These periodic changes are instead forbidden in the underlying predator-prey system. They are of neutral nature for the damaging model, may however settle to a stable equilibrium in the periodic superpredation system under suitable circumstances, and in turn give rise also to persistent limit cycles. Thus this elementary investigation elucidates a possible invasion mechanism where the moving population spots an attracting ecosystem where thriving is possible and settles in it.

References

1. Alerstam, T., Bäckman, J.: Ecology of animal migration. *Current Biology* **28** (17), R968–R972 (2018)
2. Liedvogel, M., Åkesson, S., Bensch, S.: The genetics of migration on the move. *Trends in Ecology & Evolution* **26** (11), 561–569 (2011)
3. Lohmann, K.J.: Animal migration research takes wing. *Current Biology* **28** (17), R952–R955 (2018)
4. Couzin, I.D.: Collective animal migration. *Current Biology* **28** (17), R976–R980 (2018)
5. Aikens, E.O., Bontekoe, I.D., Blumenstiel, L., Schlicksupp, A., Flack, A.:

- Viewing animal migration through a social lens. *Trends in Ecology & Evolution* **37** (11), 985–996 (2022)
6. Justen, H., Delmore, K.E.: The genetics of bird migration. *Current Biology* **32** (20), R1144–R1149 (2022)
 7. Lees, A.C., Gilroy, J.J.: Bird migration: When vagrants become pioneers. *Current Biology* **31** (24), R1568–R1570 (2021)
 8. Helm, B., Muheim, R.: Bird migration: Clock and compass facilitate hemisphere switching. *Current Biology* **31** (17), R1058–R1061 (2021)
 9. Corkeron, P.J., Van Parijs, S.M., Adamczak, S.K.: Marine Mammal Migrations and Movement Patterns. In: Cochran, J.K., Bokuniewicz, H.J., Yager, P.L. (eds) *Encyclopedia of Ocean Sciences (Third Edition)*, pp. 563–571. Academic Press (2019)
 10. Fryxell, J.M., Sinclair, A.R.E.: Seasonal migration by white-eared kob in relation to resources. *African Journal of Ecology* **26**, 17–31 (1988)
 11. Harris, G., Thirgood, S., Hopcraft, J.G.C., Cromsigt, J.P.G.M., Berger, J.: Global decline in aggregated migrations of large terrestrial mammals. *Endangered Species Research* **7**, 55–76 (2009)
 12. Fryxell, J.M., Sinclair, A.R.E.: Causes and consequences of migration by large herbivores. *Trends in Ecology & Evolution* **3** (9), 237–241 (1988)
 13. Fryxell, J.M.: Aggregation and migration by grazing ungulates in relation to resources and predators. *Serengeti II: dynamics, management, and conservation of an ecosystem* **2**, 257 (1995)
 14. Kubelka, V., Sandercock, B.K., Székely, T., Freckleton, R.P.: Animal migration to northern latitudes: environmental changes and increasing threats. *Trends in Ecology & Evolution* **37** (1), 30–41 (2022)
 15. Altizer, S., Teitelbaum, C.S., Hall, R.J.: Animal Migration and Parasitism. In: Choe, J.C. (eds) *Encyclopedia of Animal Behavior (Second Edition)*, pp. 756–763. Academic Press (2019)
 16. Reichle, D.E.: Chapter 7 - Food chains and trophic level transfers. In: Reichle, D.E. (eds) *The Global Carbon Cycle and Climate Change (Second Edition)*, pp. 129–151. Elsevier (2023)
 17. Donohue, J.G., Piironen, P.T.: Mathematical modelling of seasonal migration with applications to climate change. *Ecological Modelling* **299**, 79–94 (2015)
 18. Mose, V.N., Nguyen-Huu, T., Western, D., Auger, P., Nyandwi, C.: Modelling the dynamics of migrations for large herbivore populations in the Amboseli National Park, Kenya. *Ecological Modelling* **254**, 43–49 (2013)
 19. Huang, Z.: Migration dynamics simulation of migratory fish in rivers. *Ecological Indicators* **158**, 111293 (2024)
 20. Davey, N., Dunstall, S., Halgamuge, S.: Optimal road design through ecologically sensitive areas considering animal migration dynamics. *Transportation Research Part C: Emerging Technologies* **77**, 478–494 (2017)
 21. Sridharan, V.K., Jackson, D., Hein, A.M., Perry, R.W., Pope, A.C., Hendrix, N., Danner, E.M., Lindley, S.T.: Simulating the migration dynamics of juvenile salmonids through rivers and estuaries using a hydrodynamically driven enhanced particle tracking model. *Ecological Modelling* **482**, 110393 (2023)

22. Jiao, J., Quan, Q., Dai, X.: Dynamics of a new impulsive predator–prey model with predator population seasonally large-scale migration. *Applied Mathematics Letters* **132**, 108096 (2022)
23. Upadhyay, R.K., Naji, R.K., Raw, S.N., Dubey, B.: The role of top predator interference on the dynamics of a food chain model. *Communications in Nonlinear Science and Numerical Simulation* **18** (3), 757–768 (2013)
24. Gil-Sánchez, J.S., Sánchez-Cerdá, M.: Current overlapping distribution of megaherbivores and top predators: An approach to the last terrestrial areas with ecological integrity. *Biological Conservation* **277**, 109848 (2023)